Analysis of Ozone (O_3) and Erythemal UV (EUV) measured by TOMS in the equatorial African belt

Authors:
Taddeo Ssenyonga[1]
Jakob J. Stamnes[2]
Arne Dahlback[3]
Andreas Steigen[4]
Willy Okullo[1]
Øyvind Frette[2]

Affiliations:
[1]Department of Physics, Makerere University, Kampala, Uganda

[2]Department of Physics and Technology, University of Bergen, Bergen, Norway

[3]Department of Physics, University of Oslo, Olso, Norway

[4]Department of Biology, University of Bergen, Thormøhlensgt, Norway

Correspondence to:
Øyvind Frette

email:
oyvind.frette@ift.uib.no

Postal address:
Department of Physics and Technology, University of Bergen, Box 7803, N 5020, Bergen, Norway

Keywords:
ozone; erythemal UV; TOMS; equatorial Africa; TOCA

Dates:
Received: 27 Mar. 2009
Accepted: 09 Nov. 2009
Published: 11 Mar. 2010

How to cite this article:
Ssenyonga T, Stamnes JJ, Dahlback A, Steigen A, Okullo W, Frette Ø. Analysis of Ozone (O_3) and Erythemal UV (EUV) measured by TOMS in the equatorial African belt. S Afr J Sci. 2010;106(1/2), Art. #12, 7 pages. DOI:10.4102/sajs.v106i1/2.12

This article is available at:
http://www.sajs.co.za

ABSTRACT

We presented time series of total ozone column amounts (TOCAs) and erythemal UV (EUV) doses derived from measurements by TOMS (Total Ozone Mapping Spectrometer) instruments on board the Nimbus-7 (N7) and the Earth Probe (EP) satellites for three locations within the equatorial African belt for the period 1979 to 2000. The locations were Dar-es-Salaam (6.8° S, 39.26° E) in Tanzania, Kampala (0.19° N, 32.34° E) in Uganda, and Serrekunda (13.28° N, 16.34° W) in Gambia. Equatorial Africa has high levels of UV radiation, and because ozone shields UV radiation from reaching the Earth's surface, there is a need to monitor TOCAs and EUV doses. In this paper we investigated the trend of TOCAs and EUV doses, the effects of annual and solar cycles on TOCAs, as well as the link between lightning and ozone production in the equatorial African belt. We also compared clear-sky simulated EUV doses with the corresponding EUV doses derived from TOMS measurements. The TOCAs were found to vary in the ranges 243 DU – 289 DU, 231 DU – 286 DU, and 236 DU – 296 DU, with mean values of 266.9 DU, 260.9 DU, and 267.8 DU for Dar-es-Salaam, Kampala and Serrekunda, respectively. Daily TOCA time series indicated that Kampala had the lowest TOCA values, which we attributed to the altitude effect. There were two annual ozone peaks in Dar-es-Salaam and Kampala, and one annual ozone peak in Serrekunda. The yearly TOCA averages showed an oscillation within a five-year period. We also found that the EUV doses were stable at all three locations for the period 1979–2000, and that Kampala and Dar-es-Salaam were mostly cloudy throughout the year, whereas Serrekunda was mostly free from clouds. It was also found that clouds were among the major factors determining the level of EUV reaching the Earth´s surface. Finally, we noted that during rainy seasons, horizontal advection effects augmented by lightning activity may be responsible for enhanced ozone production in the tropics.

INTRODUCTION

Atmospheric ozone shields life at the Earth's surface from UVB (280 nm – 315 nm), the most harmful part of the solar UV radiation. UVB radiation has diverse harmful effects on the environment as a whole.[1,2,3,4] Its transmission through the stratosphere is primarily determined by the total amount of stratospheric ozone. Besides shielding the Earth from UVB radiation, ozone also plays a key role in chemical processes and for the energy budget of the troposphere (0 km – 10 km).[5,6] About 90% of the ozone resides in the stratosphere between 10 km and 50 km above the Earth's surface. According to Allen et al.[7], atmospheric ozone is the primary precursor of OH, a main radical oxidant. Therefore, ozone plays an essential role in the oxidising power of the troposphere. Hongyu et al.[8] showed that the production of atmospheric ozone takes place in the troposphere through photochemical oxidation of hydrocarbons and CO in the presence of NO_x (NO + NO_2) radicals. According to the findings of McFarland and Kaye[9], as well as Austin and Midgley[10], ozone precursors (hydrocarbons, CO, NO_x) are mainly due to human activities such as fossil fuel combustion, industrial processes, and biomass burning. In addition, there are other sources such as microbial activity in soils and volcanic eruptions.

Based on satellite observations during the period 1979–1985 in Antarctica, Stolarski et al.[11,12] reported a negative trend of TOCAs. Herman et al.[13], who also based their conclusions on satellite measurements (1979–1992), reported a significant increase in the UVB radiation due to a decrease in atmospheric ozone levels. Furthermore, Kerr and McElroy[14] reported a significant increase in the UVB radiation during the period from 1989 to 1993 in Toronto, caused by a decrease in TOCAs during the same period.

According to McPeters and Labow[15], who compared TOCAs derived from TOMS data with corresponding ground-based measurements (Dobson network), EP-TOMS derived TOCAs were about 1.0% higher than those obtained from a 30-station Dobson network of ground measurements. TOCAs derived from N7-TOMS data were about 0.5% higher than those derived from the Dobson network, and Meteor-3 TOMS data gave TOCAs that were not significantly different from those of the Dobson network. None of the TOMS-derived ozone data sets showed any significant drift relative to measurements by the ground-based networks. Liu et al.[16] reported occurrences of some anomalies in TOCAs derived from N7-TOMS and EP-TOMS Version 7 data over cloudy areas, with average fractions of TOCA anomalies derived from N7-TOMS and EP-TOMS over all cloudy areas of (31.8 ± 7.7)% and of (35.8 ± 9.7)%, respectively. Further, these anomalies were not uniformly distributed around the globe. According to Bhartia et al.[17], some uncertainties in the TOMS Version 7 algorithm were corrected in Version 8, giving improved Version 8 data products. The improvements in the Version 8 algorithm were based on: (1) aerosol/glint correction based on the aerosol index, (2) new ozone profile climatology, (3) new temperature profile climatology, (4) tropospheric ozone climatology, (5) improved surface reflectivity modelling, and (6) more accurate radiative transfer modelling.

Ozone is one of the major tropospheric gaseous compounds produced by photochemical reactions due to the byproducts of biomass burning.[18,19,20,21] Estimates showed that biomass burning is the source of 38% of tropospheric ozone on a global scale.[22] Savannah and open woodland burning during the dry season is widespread in Africa, where it is traditionally an integral part of the agricultural policy for clearing the land of old grass, shifting cultivation, and hunting. Owing to ozone´s long life

(about 3 months), it can be transported over large distances. According to Cook et al.[23], the presence of increased ozone concentrations at the surface is a good indication that locally occurring biomass burnings are emitting precursors for ozone formation. Thus, in sub-equatorial Africa, ozone precursor emissions from regional biomass burning were found to be comparable in magnitude to those due to biogenic, lightning, and anthropogenic sources.[24]

Reed[25] and Godson[26] were the first to comprehensively explain the role of the vertical motions, the accompanying stratospheric temperature changes, and the influence of long planetary waves on ozone changes. According to Baldwin et al.[27], quasi-biennial oscillations (QBOs) are downward propagating easterly and westerly wind regimes with a variable period averaging approximately 28 months. From a fluid dynamics perspective, these winds are classified as coherent, oscillating mean flows that are driven by propagating waves, with periods unrelated to those of the resulting oscillations. The QBOs are driven and modulated by atmospheric wave motions. They affect the variability of the atmospheric constituents in the mesosphere near an altitude of 85 km by selectively filtering waves that propagate upward through the equatorial stratosphere, and they may also affect the strength of Atlantic hurricanes. The effects of the QBOs are not confined to atmospheric dynamics. Chemical constituents such as ozone, water vapour, and methane, are also affected by circulation changes induced by QBOs.

Bowman[28] reported that inter-annual variations of TOCA values near the equator are dominated by QBOs, latitudinal winds and temperature, which transport ozone from the equator. Through 10 years of TOCA values derived from TOMS data over the equator, Shiotani et al.[29]found an annual cycle in total ozone, and maximum and minimum mean values of the latitudinal winds occurring around September and January, respectively.

According to Pickering et al.[30] and Thompson et al.[31], the deep convection occurring over equatorial Africa during the rainy season serves as a vertical transport mechanism for aerosols and trace gases to the middle and upper troposphere. However, these deep convections are largely absent during the dry seasons, although dry convective processes such as turbulence and 'dust devils' (small but rapidly rotating columns of wind of short duration that are made visible by dust, sand, and debris picked up from the ground) can lead to substantial vertical atmospheric motions. Furthermore, analyses of backward air parcel trajectories (based on the European Centre for Medium-Range Weather Forecasts (ECMWF) and National Meteorological Centre (NMC) data sources) indicated that nearly 70% of incoming mid-tropospheric transport during the mid-August or mid-September ozone peaks in the tropical mid-Atlantic came from the African continent.[31,32,33] The majority of which originated in equatorial Africa (10° N to 15° S), leading to seasonal variations of TOCAs across equatorial Africa.

According to Tian et al.[34], who based their study on merged ozone data sets (5° x 10° lat-lon grid), TOCAs in the tropics co-vary with the Madden-Julian Oscillation (MJO), with deviations from the mean TOCA value of about 10 DU. The strength of this co-variation is comparable to those due to the annual cycle[29] (about 10 DU), El Niño-Southern Oscillation (ENSO)[35] (about 15 DU), QBO[28] (about 15 DU), and the solar cycle[36] (about 5 DU).

Because the sun is nearly directly overhead in the equatorial belt, high levels of UV radiation are to be expected. In order to determine the ozone and EUV climatology for Dar-es-Salaam (6.8° S, 39.26° E), Kampala (0.19° N, 32.34° E), and Serrekunda (13.28° N, 16.34° W), we relied on clear-sky simulated values and TOMS-derived values because McPeters and Labow[15] showed that these were accurate. The polar-orbiting TOMS instruments have measured TOCAs and EUV doses over the entire Earth, from November 1978 to the present, except for a non-operational period from May 1993 to July 1996. In this paper we considered TOCAs and daily integrated EUV doses from 1978 to 2000. After the year 2000 there was a latitude-dependent error detected in the measurements.[37]

Ozone and EUV retrieval by TOMS and EUV simulations

According to McPeters et al.[38], TOMS instruments measure UV radiances backscattered by the underlying atmosphere, clouds and surface. The radiances measured depend on the TOCA, the vertical distribution of the ozone, the solar-zenith angle, the satellite azimuth and scan angle, the pressure level, the cloud reflectivity, and the reflectivity of the surface. All these parameters, except the TOCA, can be determined from knowledge of the satellite position, International Satellite Cloud Climatology Project (ISCCP) cloud data, and radiances measured at the wavelength of 360 nm (380 nm for N7-TOMS), where the ozone absorption is negligible. The TOMS algorithm determines the TOCA by comparing calculated radiances with measured radiances. The calculated radiances are computed by fixing all input parameters in the radiative transfer calculation and varying the TOCA. The value of the TOCA that makes the radiance calculated by the radiative transfer code equal to measured radiance is the TOCA value used for that location.

There are some uncertainties in the TOCA and daily integrated EUV dose values derived from TOMS measurements. According to the EP-TOMS user guide[38], there are three different components that determine the accuracy of the normalised radiances used in the TOCA retrieval from TOMS data: (1) the accuracy of the measured radiances, (2) the initial laboratory calibration, and (3) the time-dependent drift in the instrument sensitivity. These sources of uncertainties can further be classified as: random error, time-independent absolute error, and time-dependent drift error. For TOCAs derived from Version 7 TOMS data, the absolute error is ±3%, the random error is ±2% (but slightly increased at high latitudes), and the drift after 1.5 years of operation was less than ±0.6%. The root mean square error produced by the EP-TOMS algorithm increases with both the solar zenith angle and increased aerosol loading, and is not uniformly distributed around the globe. According to Herman et al.[39], the accuracy of the UV exposure on a particular day, at any given location, is limited by the satellite´s poor spatial resolution and the assumption that the overpass atmospheric conditions are constant for the whole day.

Our UV radiation model is based on the discrete ordinate solution of the radiative transfer equation[40], which is modified to account for the curvature of the atmosphere.[41] The model includes absorption and multiple scattering in the vertical inhomogeneous atmosphere, and the ground is treated as a Lambert reflector. The air pressure, ozone, and temperature profile were taken from the National Oceanic and Atmospheric Administration.[42] The ozone cross-sections were taken from Molina and Molina[43], and the Rayleigh-scattering cross-sections were obtained from an empirical formula by Nicolet.[44] The extraterrestrial solar spectrum used in our model was the Atlas3 solar spectrum taken from ftp://susim0.nrl.navy.mil/pub/atlas3/ in March 2001. The U=V calculations were adjusted for the eccentricity of the Earth's orbit. The time resolution of the calculated daily-integrated EUV doses was 30 min. A surface albedo of 0.05 and daily TOCAs derived from TOMS data were used in the simulations of the clear-sky daily integrated EUV doses.

RESULTS AND DISCUSSIONS

We simulated clear-sky daily integrated EUV doses and derived daily integrated EUV doses and daily TOCA values from TOMS Version 8 data sets. We then computed the yearly averages of EUV doses and TOCAs from 1979–2000 for the three locations Dar-es-Salaam, Kampala, and Serrekunda. The monthly mean $\bar{X}(iy, im)$ was calculated as follows:

$$\bar{X}(iy, im) = \frac{1}{N}\sum_{j=1}^{N} X_j \qquad \text{[Eqn 1]}$$

where $\bar{X}_j$ is the TOCA or EUV dose of the jth day of the month im, and where $j = 1$ and $j = N$ denote the beginning and end dates of the month im and year iy. Months which had fewer than 75% of days with data were not considered in these computations. The yearly averages were computed by averaging the monthly mean values for each particular year. Years which had no data for any of the 12 months were also not considered. The Dar-es-Salaam station was selected because of its proximity to the ocean, Kampala because of its far inland location, and Serrekunda because of its proximity to the Sahara Desert.

Figures 1, 2 and 3 (which have gaps due to a non-operational 3-year period from May 1993 to July 1996 for the TOMS satellite

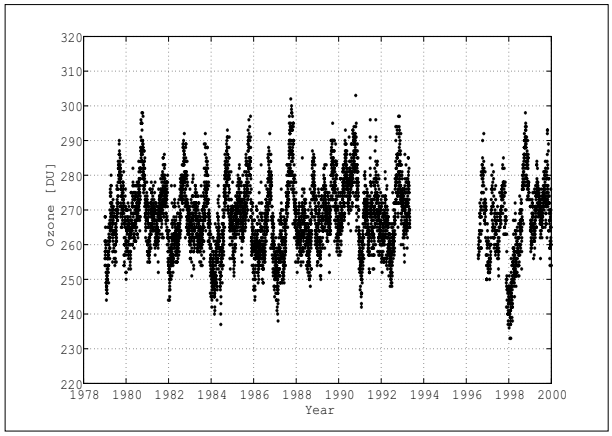

FIGURE 1
Time series of daily TOCAs derived from TOMS data for Dar-es-Salaam for the period 1979 to 2000

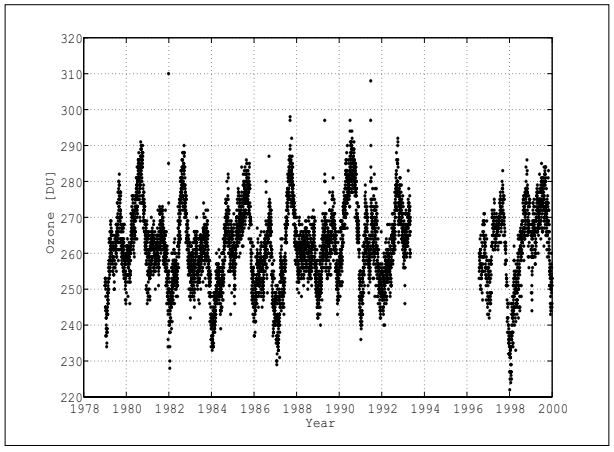

FIGURE 2
Time series of daily TOCAs derived from TOMS data for Kampala for the period 1979 to 2000

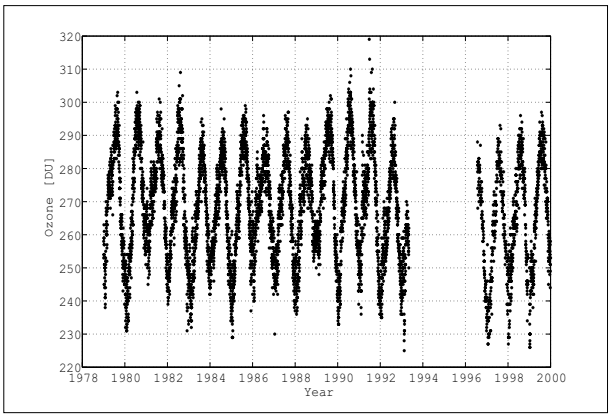

FIGURE 3
Time series of daily TOCAs derived from TOMS data for Serrekunda for the period 1979 to 2000

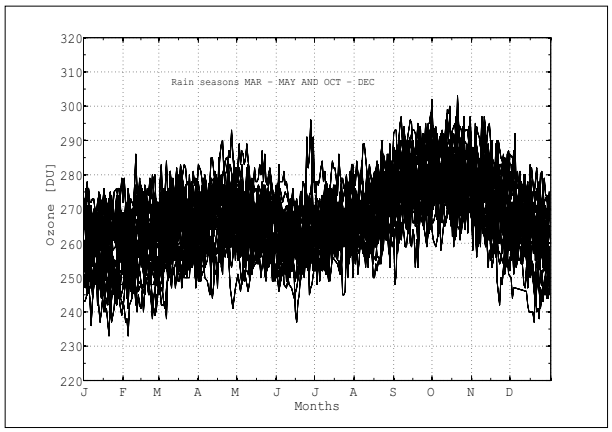

FIGURE 4
Daily variations of TOCAs derived from TOMS data for Dar-es-Salaam for all years from 1979 to 2000

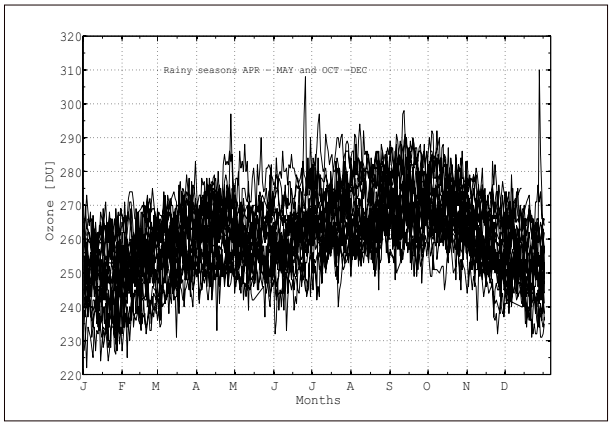

FIGURE 5
Daily variations of TOCAs derived from TOMS data for Kampala for all years from 1979 to 2000

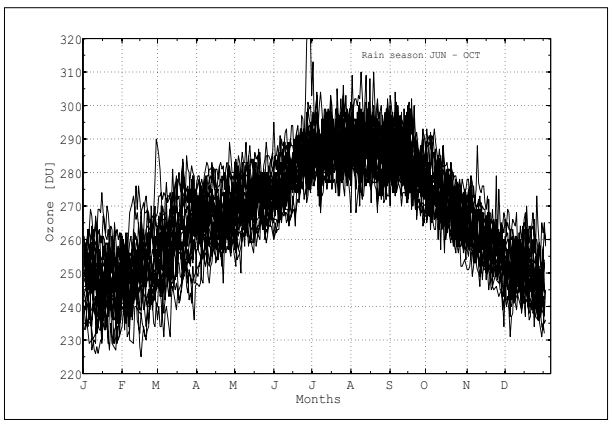

FIGURE 6
Daily variations of TOCAs derived from TOMS data for Serrekunda for all years from 1979 to 2000

instruments) show time series of daily TOCA values, which vary from 233 DU to 303 DU for Dar-es-Salaam, from 222 DU to 310 DU for Kampala, and from 225 DU to 329 DU for Serrekunda. The mean values ± standard deviations are 267.2 ± 10.31 DU, 261 ± 11.3 DU, and 268.1 ± 15.97 DU for Dar-es-Salaam, Kampala, and Serrekunda, respectively. The standard deviations are similar to those found in TOCA studies to determine the effects of the annual cycle (±10 DU)[12], QBO (±15 DU)[28], solar cycle (±5 DU)[36], and MJO (±10 DU).[34] The interannual variations of TOCAs in Figures 1-3 may be due to quasibiennial oscillations (QBOs)[28],

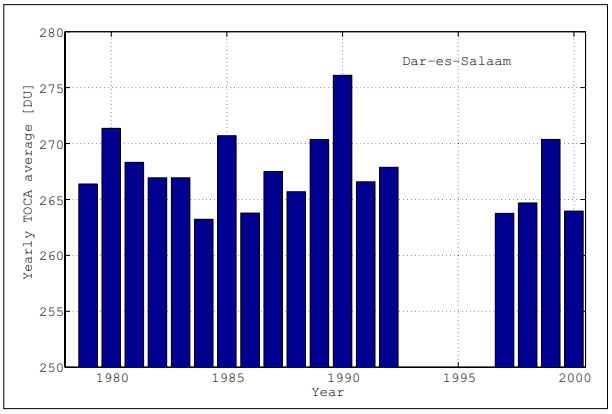

FIGURE 7a
Yearly averages of TOCA values for Dar-es-Salaam, derived from TOMS data for the period 1979 to 2000

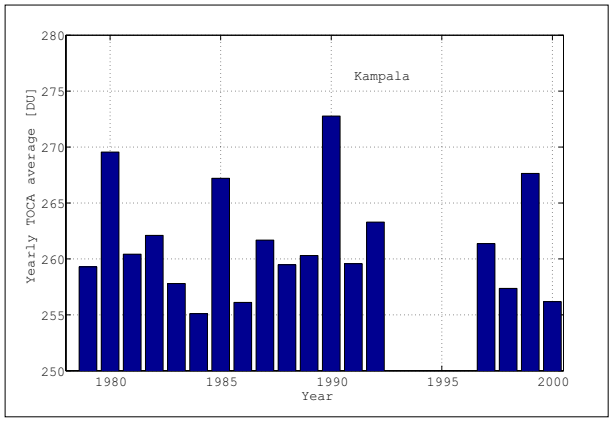

FIGURE 7b
Yearly averages of TOCA values for Kampala derived from TOMS data for the period 1979 to 2000

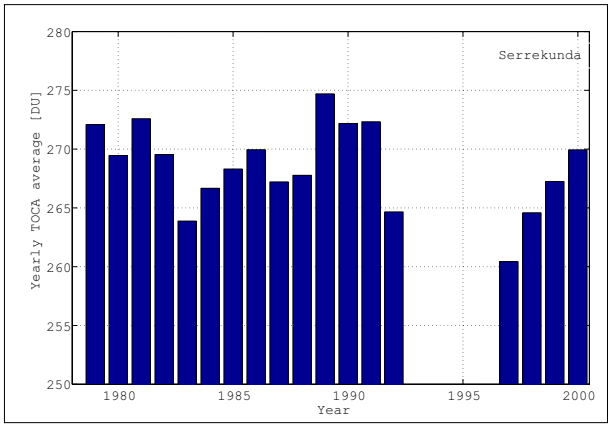

FIGURE 7c
Yearly averages of TOCA values for Serrekunda derived from TOMS data for the period 1979 to 2000

the annual cycle[29] or the ENSO.[35] Bowman[28] used nine years of total ozone measurements by N7-TOMS to show that the interannual variations of TOCAs near the equator are dominated by QBOs. Similar findings for tropical TOCAs were obtained by Logan et al.[45] based on *in situ* measurements by ozonesondes, supplemented by satellite ozone-profile and column data.

Figures 4, 5, and 6 show daily variations of the TOCA for Dar-es-Salaam, Kampala, and Serrekunda, respectively. TOCAs are plotted against month for each of the years 1979–2000. We see that Dar-es-Salaam and Kampala experience two ozone peaks per year, while Serrekunda experiences one ozone peak per year. In this context, it is worth noting that both Dar-es-Salaam and Kampala have two rainy seasons: March-May and October-December in Dar-es-Salaam and April-May and October-November in Kampala. Serrekunda has only one rainy season, from June to October. Figures 4, 5, and 6 show that the two ozone peaks per year for Dar-es-Salaam and Kampala and the single ozone peak per year for Serrekunda, all occur during the rainy seasons. Annual ozone variations originate principally at altitudes between 5 km – 20 km, where photochemical effects are negligible[46,47] and are attributed to the effects of horizontal advection or large-scale vertical motions of latitudinal winds[25], which might be related to the occurrence of rainy seasons. The variability is seen to be greater in Kampala than at the other two stations, which might be because Kampala is cloudier throughout the year. As discussed by Liu et al.[48], anomalies occur in ozone distributions derived from Nimbus-7 and Earth-Probe TOMS Version 7 data over cloudy areas.

According to Cros et al.[21] and Bond et al.,[49] ozone peaks are partly due to seasonal variations in biomass burning, and partly due to lightning, or biogenic and anthropogenic sources. In the three locations investigated here, the ozone peaks occurred during rainy seasons, when there was little biomass burning, but significant lightning. Thus, if biogenic and anthropogenic sources of ozone precursors were the same throughout the year and horizontal advection played no role, increased lightning activity would contribute to the ozone peaks during the rainy seasons, but because tropospheric ozone constitutes only about 10% of the TOCA, this contribution would not be very significant. Assuming no significant annual variation in anthropogenic sources and no significant contribution from biomass burning during the rainy season, we concluded that the ozone peaks probably are due to horizontal advection effects that are enhanced by lightning activity.

Figure 7 (with gaps for the same reason as for Figures 1–3) shows yearly averages of TOCAs derived from TOMS data for Dar-es-Salaam, Kampala, and Serrekunda. The yearly averages and standard deviations, as well as minimum and maximum values of TOCAs are shown in Table 1. The yearly average is altitude dependent. Kampala, which is at an elevation of about 1 200 m above sea level, has the lowest yearly TOCA average of 261.3 DU, whereas Dar-es-Salaam and Serrekunda, which are at sea level, have higher values, of 267.2 DU and 268.1 DU, respectively. From Figure 7 we also see that the maximum values of the yearly averages of the TOCA for Dar-es-Salaam and Kampala occur in 5-year intervals (1980, 1985, 1990, and 1999), which indicates an oscillation with a period of five years. Also, we noted that the lowest TOCA value in Dar-es-Salaam and Kampala occurred in 1984, in agreement with Indeje and

TABLE 1
Yearly average TOCAs derived from TOMS data for Dar-es-Salaam, Kampala and Serrekunda

	TOCA (DU)			
Location	Minimum	Maximum	Average	Standard Deviation(%)
Dar-es-Salaam	263.2	276.1	267.2	3.252
Kampala	255.1	272.8	261.3	4.812
Serrekunda	260.4	274.7	268.1	3.685

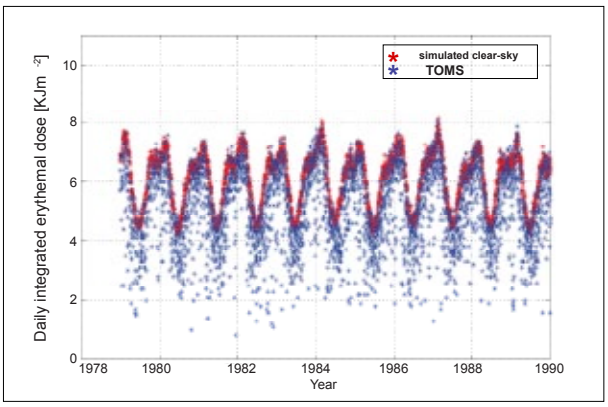

FIGURE 8a
Time series of the simulated clear-sky daily integrated EUV doses and corresponding TOMS-derived daily integrated EUV doses for Dar-es-Salaam for the period 1979 to 1990

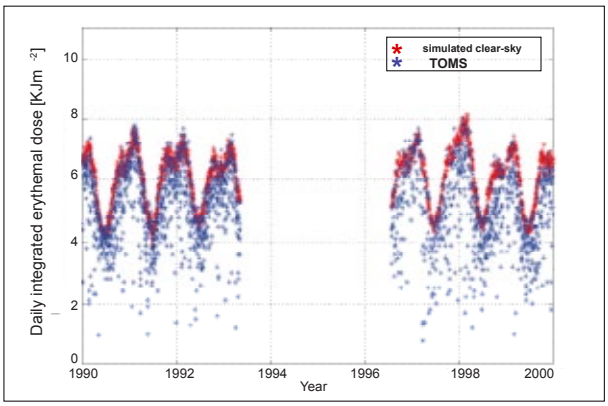

FIGURE 8b
Time series of the simulated clear-sky daily integrated EUV doses and corresponding TOMS-derived daily integrated EUV doses for Dar-es-Salaam for the period 1990 to 2000

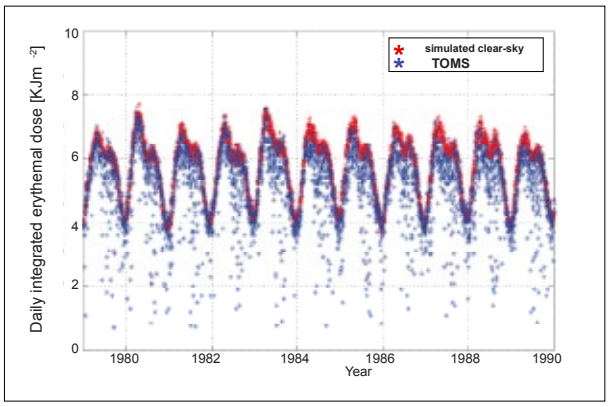

FIGURE 9a
Time series of the simulated clear-sky daily integrated EUV doses and corresponding TOMS-derived daily integrated EUV doses for Serrekunda for the period 1979 to 1990

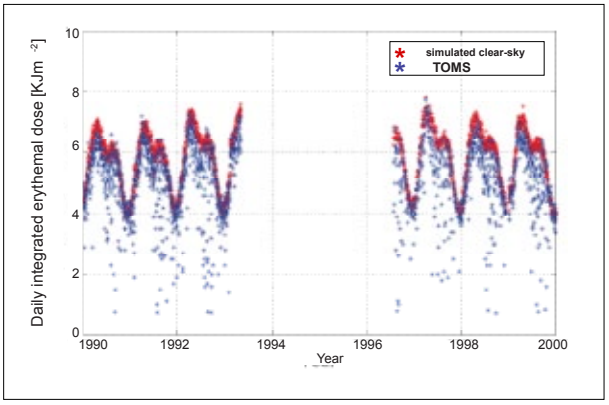

FIGURE 9b
Time series of the simulated clear-sky daily integrated EUV doses and corresponding TOMS-derived daily integrated EUV doses for Serrekunda for the period 1990 to 2000

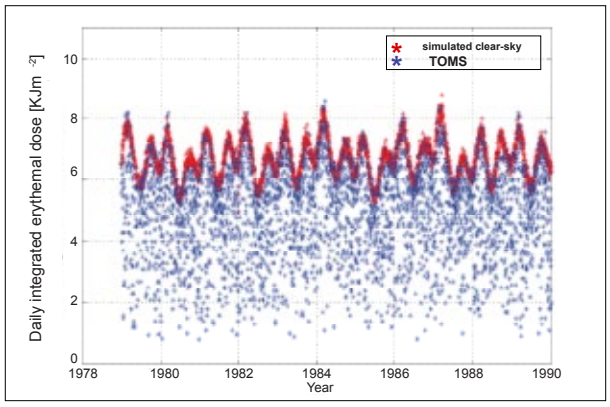

FIGURE 10a
Time series of the simulated clear-sky daily integrated EUV doses and corresponding TOMS-derived daily integrated EUV doses for Kampala for the period 1979 to 1990

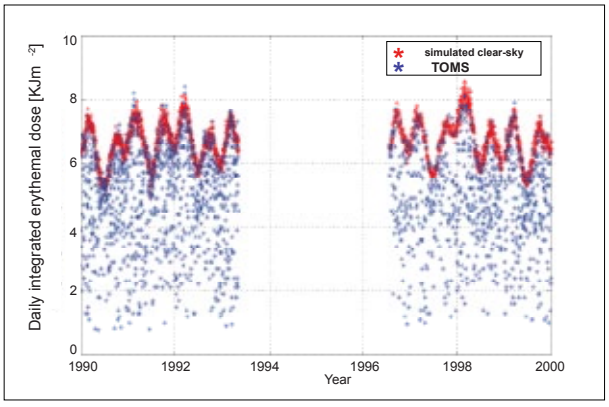

FIGURE 10b
Time series of the simulated clear-sky daily integrated EUV doses and corresponding TOMS-derived daily integrated EUV doses for Kampala for the period 1990 to 2000

Semazzi[50], who noted that 1984 experienced the strongest ENSO of the century. It will be of interest in future studies to see whether this 5-year oscillation will continue over a longer time span, and, if so, it may be beneficial to investigate the underlying mechanisms causing it.

In Figures 8–10 (with gaps for the same reason as for Figures 1–3), we compared the simulated clear-sky daily integrated EUV doses with the corresponding daily integrated EUV doses derived from TOMS data. The simulated clear-sky results compared favourably with the TOMS-derived results for Serrekunda (Figure 9), whereas simulated clear-sky results and TOMS-derived results were not in agreement for Kampala (Figure 10) and Dar-es-Salaam (Figure 8). The good agreement for Serekunda is due to the fact that about 80% of the days throughout the year are clear,[51] whereas Kampala and Dar-es-Salaam are mostly cloudy throughout the year. Also, we see from Figures 8–10 that the simulations agree well with the TOMS-derived results at the peaks, which is expected because the simulations represent clear-sky days when the EUV doses

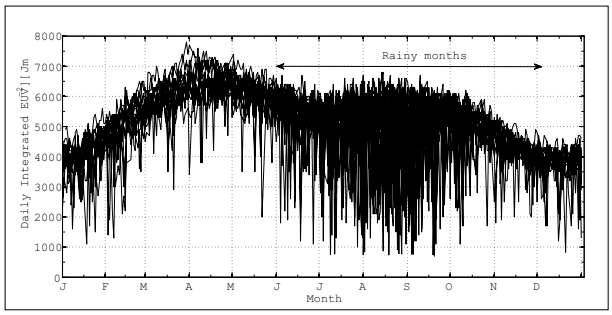

FIGURE 11
Daily variations of daily integrated EUV doses derived from TOMS data for Serrekunda from 1979 to 2000

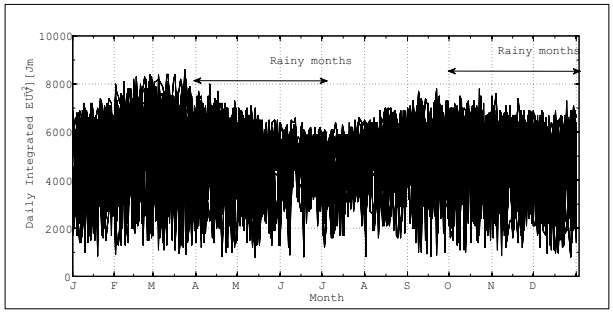

FIGURE 12
Daily variations of daily integrated EUV doses derived from TOMS data for Kampala from 1979 to 2000

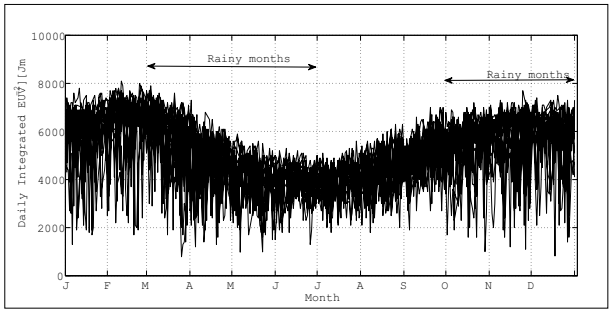

FIGURE 13
Daily variations of daily integrated EUV doses derived from TOMS data for Dar-es-Salaam from 1979 to 2000

are highest. The annual averages of daily integrated EUV doses for Kampala, Dar-es-Salaam and Serrekunda are quite stable around 5 kJ/m^2. These averages are five times larger than the 14-year average of daily integrated EUV doses measured in Oslo, Norway at 60 °N.[52]

Figures 11–13 show daily integrated EUV doses for Serrekunda, Kampala and Dar-es-Salaam, respectively. Figure 11 shows that the largest variations occur during the rainy season in Serrekunda, and since rain removes aerosols from the atmosphere, these variations are due to cloud effects. Because Kampala and Dar-es-Salaam are cloudy throughout the year, the correlation between rainy season and daily integrated EUV is poor, as shown in Figures 12 and 13.

Plots of yearly averages of daily integrated EUV doses (not shown) indicated that these were fairly stable at all three locations during the period from 1979 to 2000. Thus, the mean yearly average and the standard deviation of the daily integrated EUV dose were found to be 5.13 ± 0.12 kJ/m^2 for Dar-es-Salaam, 5.02 ± 0.19 kJ/m^2 for Kampala, and 5.12 ± 0.09 kJ/m^2 for Serrekunda. Also, we compared plots (not shown) of TOCAs derived from TOMS data based on the Version 7 algorithm with those based on the new Version 8 algorithm for Serrekunda for the period 1979–2000. We found that the average ratio of the TOCAs derived from that TOMS data was 1.01 with a standard deviation of 1.6%. If we accept the results as correct, Version 7 therefore, on average, underestimates TOCAs for Serrekunda by 1%. As discussed earlier, the difference is attributed to the improvement of the Version 8 TOMS data processing algorithm.[17]

CONCLUSION

We derived daily integrated EUV doses and TOCA values from TOMS data for the equatorial African belt for locations in Kampala (Uganda), Dar-es-Salaam (Tanzania), and Serrekunda (Gambia). Our findings showed that:

- Dar-es-Salaam and Kampala experienced two ozone peaks per year, whereas Serrekunda experienced one ozone peak per year. The peaks occurred in rainy seasons, and are probably due to horizontal advection effects that were enhanced by lightning activity.
- The inter-annual oscillations of the TOCAs are about 10 DU, about 11 DU, and about 16 DU for Dar-es-Salaam, Kampala, and Serrekunda, respectively. These are in agreement with observations by Shiotani[29], Bowman et al.[28] and Hood[36].
- There was a reduction in TOCAs during the dry seasons for all three locations (Serrekunda, Kampala and Dar-es-Salaam). These reductions are attributed to latitudinal oscillations, which exist during the dry season, and they are in agreement with the findings of Thompson et al.[31], Fuelberg et al.[32], Swap et al.[33], Tian et al.[34] and Di Sarra et al.[53]
- Kampala and Dar-es-Salaam were mostly cloudy throughout the year, whereas Serrekunda had many clear-sky days throughout the year, in agreement with Herman et al.[51]
- Besides TOCA values, clouds are among the major factors determining the levels of EUV reaching the Earth´s surface.
- The mean yearly average of the daily integrated EUV dose was found to be fairly stable at the three locations during the period from 1979 to 2000, with mean values and standard deviations of 5.13 ± 0.12 kJ/m^2 for Dar-es-Salaam, 5.02 ± 0.19 kJ/m^2 for Kampala, and 5.12 ± 0.09 kJ/m^2 for Serrekunda.
- Finally, the ratio between TOCAs derived from TOMS data based on algorithm Version 8 and algorithm Version 7 indicated that algorithm Version 7 underestimates TOCAs for Serrekunda by 1%.

ACKNOWLEDGEMENTS

We wish to thank the TOMS Ozone Processing Team for making the TOMS ozone data available publicly. Also, we would like to acknowledge support from the Norwegian State Educational Loan Foundation and NUFU project 33/02.

REFERENCES

1. Caldwell MM, Björn LO, Bornman JF, et al. Effects of increased solar ultraviolet radiation on terrestrial ecosystems. Photochem Photobiol. 1998;46:40–52.
2. Searles PS, Flint SD, Caldwell MM. A meta-analysis of plant field studies simulating stratospheric ozone depletion. Oecologia. 2001;127:1–10.
3. Urbach, F. Ultraviolet radiation and skin cancer of humans. Photochem Photobiol. 1997;40:3–7.
4. De Fabo EC, Noonan FP, Frederick JE. Biologically effective doses of sunlight for immune suppression at various latitudes and their relationship to changes in stratospheric ozone. Photochem Photobiol. 1990;52:811–817.
5. Brasseur GP, Kiehl JT, Muller JF, et al. Past and future changes in global tropospheric ozone: Impact on radiative forcing. Geophys Res Lett. 1998;25:3807–3810.
6. Crutzen PJ. Tropospheric ozone: An overview, in tropospheric ozone, regional, and global scale interaction. NATO ASI Ser. 1998;25:3–32.
7. Allen DJ, Rood RB, Trompson AM, Hudson RD. Three-dimensional radon 222 calculations using assimilated meteorological data and a convective mixing algorithm. J Geophys Res. 1996;101:6871-6881.

8. Hongyu L, Daniel JJ, Yin C, et al. Sources of tropospheric ozone along the Asian Pacific Rim: An analysis of ozone sonde observations. J Geophys Res. 2002;107.
9. McFarland M, Kaye J. Chlorofluorocarbons and ozone. Photochem Photobiol. 1992;55:911–929.
10. Austin JF, Midgley RP. The climatology of the jet stream and stratosphere intrusions of ozone over Japan. Atmos Environ. 1994;28:39–52.
11. Stolarski RS, Krueger AJ, Schoeberl MR, McPeters RD, Newman PA, Alpert JC. Nimbus 7 satellite measurements of the spring time Antarctic ozone decrease. Nature. 1986;322:808–811.
12. Stolarski RS, Bojkov R, Bishop L, Zerefos C, Staehelin J, Zawodny J. Measured trends in stratospheric ozone. Science. 1992;256:342–349.
13. Herman JR, Bhartia PK, Ziemke J, Ahmad Z, Larko D. UV-B increases (1979–1992) from decreases in total ozone. Geophys Res Lett. 1996;23:2117–2120.
14. Kerr JB, McElroy CT. Evidence for large upward trends of ultraviolet-B radiation linked to ozone depletion. Science. 1993;262:1032–1034.
15. McPeters RD, Labow GJ. An assessment of the accuracy of 14.5 years of Nimbus 7 TOMS Version 7 ozone data by comparison with the Dobson network. Geophys Res Lett. 1996;23:3695–3698.
16. Liu X, Newchurch MJ, Kim JH. Occurrence of ozone anomalies over cloudy areas in TOMS version 7 level 2 data. Atmos. Chem Phys. 2003:3:187–223.
17. Bhartia PK, Wellemeyer CG, Taylor SL, Nath N, Gopolan A. Solar Backscatter Ultraviolet (SBUV) version 8 profile algorithm. Proceedings of the XX quadrennial ozone symposium; 2004 1-8 June; Kos, Greece. edited by C.S. Zerefos. Int. Ozone Comm., Athens. 2004;1:295–296.
18. Crutzen PJ, Andreae MO. Biomass burning in the tropics: Impact on atmospheric chemistry and biogeochemical cycles. Science. 1990;250:1669–1678.
19. Andreae MO, Chapuis A, Cros B, et al. Ozone and Aitken nuclei over equatorial Africa: Airborne observations during DECAFE 88. J Geophys Res. 1992;97:6137–6148.
20. Lopez A, Huertas ML, Lacome JM. Numerical simulation of the ozone chemistry observed over forested tropical areas during DECAFE experiments. J Geophys Res. 1992;97:6149–6158.
21. Cros B, Ahoua B, Orange D, Dimbele M, Lacaux JP. Tropospheric ozone on both sides of the equator in Africa. In: Levine JS, editor. Biomass Burning and Global Change. Cambridge: MIT Press, 1996.
22. Andreae MO. Biomass burning: Its history, use and distribution and its impact on environmental quality and global climate. In: Levine JS, editor. Global Biomass Burning, Atmospheric Climatic and Biospheric Implications. Cambridge: MIT Press, 1991; p. 1–21.
23. Cooke WF, Koffi B, Grégoire JM. Seasonality of vegetation fires in Africa from remote sensing data and application to a global chemistry model. J Geophys Res. 1996;101:21051–21065.
24. Swap RJ, Szuba TA, Garstang M, Annegarn HJ, Marufu L, Piketh SJ. Spatial and temporal assessment of sources contributing to the annual austral spring mid-tropospheric ozone maxima over the tropical South Atlantic. Global Change Biol. 2003;9:336–345.
25. Reed RJ. The role of vertical motions in ozone-weather relationships. J Meteor. 1950;7:263–267.
26. Godson WL. Total ozone and the middle stratosphere over the arctic and subarctic areas in winter and spring. Q J Roy Meteor Soc. 1960;86:301–317.
27. Baldwin MP, Gray LJ, Dunkerton TJ, et al. The Quasi-biennial Oscillation. Reviews of Geophysics. 2001;39:179–229.
28. Bowman KP. Global patterns of the quasi-biennial oscillation in total ozone. J Atmos Sci. 1989;46:3328–3343.
29. Shiotani M. Annual, quasi-biennial, and El Niño-Southern Oscillation (ENSO) time-scale variations in equatorial total ozone. J Geophys Res. 1992;97:7625–7633.
30. Pickering KE, Thompson AM, Wang Y, et al. Convective transport of biomass burning emissions over Brazil during TRACE A. J Geophys Res. 1996;101:23993–24012.
31. Thompson AM, Diab RD, Bodeker GE, et al. Ozone over southern Africa during SAFARI-92/TRACE A. J Geophys Res. 1996;101:23793–23808.
32. Fuelberg HE, VanAusdall JD, Browell EV, Longmore SP. Meteorological conditions associated with vertical distributions of aerosols off the west coast of Africa. J Geophys Res. 1996;101:24105–24115.
33. Swap R, Garstang M, Macko SA, et al. The long-range transport of southern African aerosols to the tropical South Atlantic. J Geophys Res. 1996;101:23777–23792.
34. Tian B, Yung YL, Waliser DE, et al. Intraseasonal variations of the tropical total ozone and their connection to the Madden-Julian Oscillation. Geophys Res Lett. 1988;34, doi:10.1029/2007GL029451.
35. Camp CD, Roulston MS, Yung YL. Temporal and spatial patterns of the interannual variability of total ozone in the tropics. Geophys Res Lett. 2003;108, doi:10.1029/2001JD001504.
36. Hood LL. The solar cycle variation of total ozone: Dynamical forcing in the lower stratosphere. J Geophys Res. 1997;102:1355–1370.
37. TOMS, 2004. Available from: http://toms.gsfc.nasa.gov/news/news.html
38. McPeters RD, Bhartia PK, Krueger A, et al. Earth Probe Total Ozone Mapping Spectrometer (TOMS) data products user's guide. Greenbelt, Maryland. NASA Technical Publication 206895. 1998.
39. Herman JR, Krotkov N, Celarier E, and Labow G. The distribution of UV radiation at the Earth's Surface from TOMS measured UV-backscattered radiances. J Geophys Res. 1999;104:12059–12076.
40. Stamnes K, Tsay S-C, Wiscombe W, Jayaweera K. Numerically stable algorithm for discrete-ordinate-method for radiative transfer in multiple scattering and emitting layered media. Appl Opt. 1988;27:2502–2509.
41. Dahlback A, Stamnes K. A new spherical model for computing the radiation field available for photolysis and heating rate at twilight. Planet Space Sci. 1991;39:671–683.
42. U. S. A. F. NASA. U. S. Standard Atmosphere 1976, U. S. Air Force, Gov. Print. Off., Washington, D.C., 1976 Available from: http://modelweb.gsfc.nasa.gov/atmosus_standard.html.
43. Molina LT, Molina MJ. Absolute absorption cross sections of ozone in the 185- to 350-nm wavelength range. J Geophys Res. 1986;91:501–514.
44. Nicolet M. On the molecular scattering in the terrestrial atmosphere: An empirical formulae for its calculation in the homosphere. Planet Space Sci. 1984;32:1467–1468.
45. Logan JA, Jones DBA, Megretskaia IA, et al. Quasi-biennial oscillation in tropical ozone as revealed by ozone sonde and satellite data. J Geophys Res. 2003;108:4244, doi:10.1029/2002JD002170.
46. Wulf OR, Deming L. S. The theoretical calculation of the distribution of photochemically-formed ozone in the atmosphere. Terr Magn Atmos Elect. 1936:41:199–310.
47. Wulf OR, Deming LS. The distribution of atmospheric ozone equilibrium with solar radiation and the rate of maintenance of the distribution. Terr Magn atmos Elect. 1937;42:195–202.
48. Liu X, Newchurch MJ, Kim JH. Occurrence of ozone anomalies over cloudy areas in TOMS version 7 level 2 data. Atmos Chem Phys. 2003;3:1113–1129.
49. Bond DW, Steiger S, Zhang RY, Tie XX, Orville RE. The importance of NOx production by lightning in the tropics. Atmos Environ. 2002;36:1509–1519.
50. Indeje M, Semazzi FHM. Relationships between QBO in the lower equatorial stratospheric zonal winds and East African seasonal rainfall. Meteorol Atmos Phy. 2000;73:227–224.
51. Herman JR, Celarier E, Larko D. UV 380 nm reflectivity of the Earth´s surface, clouds and aerosols. J Geophys Res. 2001;106:5335–5352.
52. Lund Myhre C, Edvardsen K, Stebel K, et al. Monitoring of the atmospheric ozone layer and natural ultraviolet radiation, Annual Report 2008. OR 29/2008, 2009;ISSN 0807-7207.
53. Di Sarra A, Cacciani M, Chambard P, et al. Effects of desert dust and ozone on the ultraviolet irradiance at the Mediterranean island of Lampedusa during PAUR II. J Geophys Res. 2002;107:8135, doi:10.1029/2000JD000139.